Journal of Alloys and Compounds 509 (2011) 10007–10013

Contents lists available at ScienceDirect

Journal of Alloys and Compounds

journal homepage: www.elsevier.com/locate/jallcom

Effects of illumination on capacitance characteristics of Au/3C-SiC/*p*-Si/Al diode

K.S. Kim [a], R.K. Gupta [b,*], G.S. Chung [a], F. Yakuphanoglu [c,d]

[a] School of Electrical Engineering, University of Ulsan, San 29, Mugeodong, Namgu, Ulsan 680-749, South Korea
[b] Department of Physics, Astronomy, and Materials Science, Missouri State University, Springfield, MO 65897, USA
[c] Metallurgical and Materials Engineering Department, Firat University, Elazig, Turkey
[d] Department of Physics and Astronomy, College of Science, King Saud University, Riyadh, Saudi Arabia

ARTICLE INFO

Article history:
Received 25 May 2011
Received in revised form 28 July 2011
Accepted 1 August 2011
Available online 10 August 2011

Keywords:
Poly 3C-SiC
Diode
Photocapacitance
Ideality factor
Barrier height

ABSTRACT

Au/3C-SiC/*p*-Si/Al Schottky barrier diode was prepared using atmospheric pressure chemical vapor deposition technique. The device parameters such as barrier height, ideality factor, and series resistance were calculated using current–voltage characteristics, and were found to be 0.44 eV, 1.55, and $1.02 \times 10^4\ \Omega$, respectively. The photocapacitive properties of the diode were studied under various illumination intensities. The transient photocapacitance measurements indicate that the capacitance of the Au/3C-SiC/*p*-Si/Al Schottky diode is very sensitive to illumination. The photocapacitance of the diode increases with increase in illumination intensity. The increase in photocapacitance with increase in illumination intensity suggests that these devices could be utilized as a photocapacitive sensor for optical sensors.

1. Introduction

Silicon carbide is a wide bandgap semiconductor with high chemical stability, high mechanical strength, good thermal, and radiation stability [1–4]. These unique properties make silicon carbide technologically very promising material for fabrication of devices which can successfully operate in harsh environment such as high voltage rectifiers, UV-radiation detectors, high temperature gas sensors [5,6]. Silicon carbide exists in different forms and among them cubic polytype silicon carbide (3C-SiC) is very important because of its low temperature synthesis (1473–2273 K) compared to hexagonal polytype (2473–2773 K), and high electron mobility ($\sim$1000 $cm^2/V\,s$) [1]. These unique properties of 3C-SiC have attracted considerable research interest for device fabrication as it can be also grown on variety of substrates [5,7].

The performance of such devices strongly depends on the quality of the metal–silicon carbide interface [7]. The device characteristics can be modified by interface surface morphology, crystallinity, and defect density of silicon carbide [8]. The effect of annealing by ArF excimer laser on the diode characteristics of 3C-SiC/Si was studied [9]. It was observed that annealing with 1–3 pulsed improves the reverse current and the ideality factor of the diode. Metal oxide semiconductor field effect transistors (MOSFETs) based on 3C-SiC on silicon substrate showed that the leakage current of the *p–n* junction was proportional to the staking fault density [10]. The electrical properties of Au/3C-SiC/*n*-Si/Al Schottky junction were reported recently [11]. The observed high ideality factor in the diode was explained on the basis of charge transport mechanism.

Recently, the structural stability as well as electronic, and optical properties of intrinsic 3C-SiC and Ni-doped 3C-SiC were studied by the first principles calculation [12]. It was observed that for the Ni-doped 3C-SiC, substitution of Ni in Si sub-lattice is energetically more favorable than that in C sub-lattice. The photoresponse of the silicon carbide based materials shows some interesting results [13]. These photodiodes displayed a low dark current and had an optical gain of $\sim$97 under illumination. Sheng et al. [14] have fabricated a photoconductive power switching device based on 3C-SiC using chemical vapor deposition technique. The ratio of the off-state resistance and on-state resistance was $\sim 10^5$, with the switching efficiency of 52%.

In present study for the first time, we report the photocapacitive response properties of Au/3C-SiC/*p*-Si/Al diode under various illuminations. In addition, various device parameters were investigated using current–voltage (*I–V*) and capacitance–voltage–frequency (*C–V–f*) studies.

2. Experimental details

Poly 3C-SiC thin films were grown on *p*-type Si substrates using atmospheric pressure chemical vapor deposition (APCVD) technique. The detail procedure can be found in previous study [11]. Briefly, 5 SLM (Standard Liter per Minute) of Ar, 1

* Corresponding author. Tel.: +1 417 8366298; fax: +1 417 8366226.
E-mail addresses: ramguptamsu@gmail.com (R.K. Gupta), fyhanoglu@firat.edu.tr (F. Yakuphanoglu).

0925-8388/$ – see front matter © 2011 Elsevier B.V. All rights reserved.
doi:10.1016/j.jallcom.2011.08.012

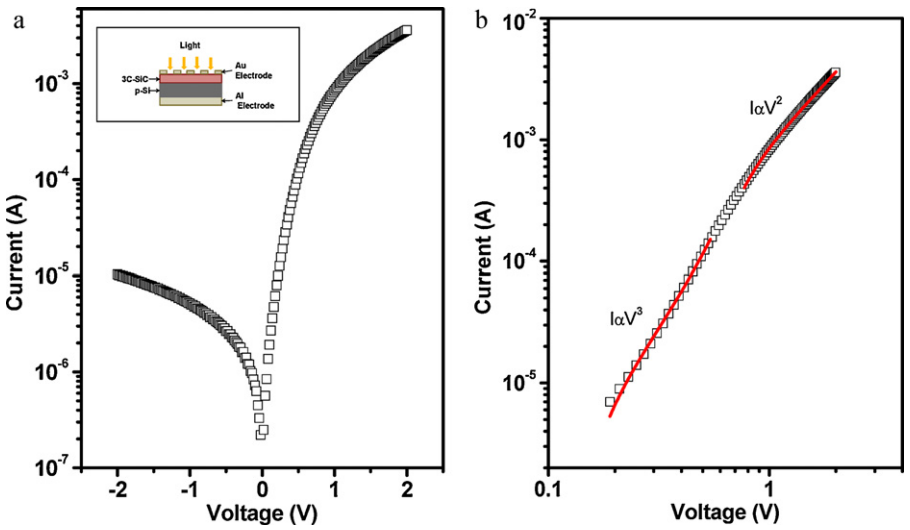

Fig. 1. (a) *I–V* characteristics of the Au/3C-SiC/*p*-Si/Al Schottky diode (inset figure shows the schematic diagram of the fabricated diode) and (b) *I–V* characteristics in logarithmic scale.

SLM of H_2 and 1 SCCM (Standard Cubic Centimeter per Minute) of $Si_2(CH_3)_6$ (HMDS) were passed for 30 min to deposit the film. The growth temperature was 1200 °C. The thickness of poly 3C-SiC was measured by atomic force microscope (AFM) and was found to be 300 nm. The Schottky contact was fabricated with gold (Au) deposition on the surface of poly 3C-SiC using direct current (DC) sputtering. The diameter and thickness of the Au contacts were 1 mm and 500 nm, respectively. Al was deposited on the back of Si substrate for ohmic contact. The ohmic contact was achieved by vacuum annealing at 400 °C for 30 min. After deposition of Al contact, Au contact was prepared and the thickness of the Au contact was measured by thickness monitor and obtained to be 150 nm. The current–voltage and capacitance–voltage characteristics of the Au/3C-SiC/*p*-Si/Al diode were performed with KEITHLEY 4200 semiconductor characterization system. Photocapacitive measurements were performed using a 200 W halogen lamp. The light intensity of the lamp was controlled by change of the current across the lamp and the intensity of light was measured using a solar power meter (TM-206).

3. Results and discussion

3.1. DC current–voltage characteristics of the Au/3C-SiC/p-Si/Al diode

The *I–V* characteristics of the Au/3C-SiC/*p*-Si/Al diode at room temperature are shown in Fig. 1(a). As seen in Fig. 1(a), the diode shows rectification behavior. The rectification ratio at ±2.0 V was found to be 351. The charge transport mechanism in such rectifying diodes can be analyzed by thermionic emission theory [15]

$$I = I_o \exp\left(\frac{q(V - IR_S)}{nkT}\right)\left[1 - \exp\left(-\frac{q(V - IR_S)}{kT}\right)\right] \quad (1)$$

where V is the applied voltage, q is the electronic charge, n is the ideality factor, k is the Boltzmann constant, T is the absolute temperature, R_S is the series resistance and I_o is the reverse saturation current. The reverse saturation current I_o is expressed by the following equation [16]

$$I_o = AA^*T^2 \exp\left(\frac{-q\phi_b}{kT}\right) \quad (2)$$

where A is the active device area, A^* is the effective Richardson constant (81.6 A cm^{-2} K^{-2} for 3C-SiC) [11] and ϕ_b is the barrier height [17]. The ideality factor and barrier height of the diode were determined and found to be 1.55 and 0.44 eV, respectively. A barrier height of 0.51 eV was reported for the Cu/pyronine-B/*p*-Si Schottky diode [18]. Hanselaer et al. [19] have studied the influence of pre-evaporation surface treatments on the electrical characteristics of *p*-Si/Au diodes. The barrier height of 0.67 eV with an ideality factor of 2.81 were reported for *p*-Si/Au diode. The higher value of ideality factor, compare to ideal value of 1, shows that the diode exhibit a non-ideal behavior. The higher value of the ideality factor shows the presence of inhomogeneities of Schottky barrier height and existence of interface states, oxide layer on silicon wafer and series resistance [20]. The ideality factor of 1.70 was observed for SiC/*p*-Si heterostructures fabricated using molecular beam epitaxy [21]. It was observed that the device fabricated on germanium-modified Si substrate improves the ideality factor to 1.36. Lebedev et al. [22] have reported higher ideality factor (>2) for *p*-3C-SiC/*n*-6H-SiC heterojunctions.

The obtained higher ideality factor suggests that the transport properties of the device could not be well defined by thermionic emission. To better understand the mechanism that controls the transport properties of the diode, log *I*–log *V* plot for the diode is shown in Fig. 1(b). The charge transport mechanism was analyzed by $I = kV^m$ relation, here m is an exponent which determines the charge transport mechanism. At higher voltages, the log *I*–log *V* plot shows two regions with different exponents. In the first region, the current is changed with V^3. This suggests that the conduction mechanism is due to exponential distribution of the traps. Whereas, in the second region, the conduction mechanism is controlled by space charge limited current (SCLC) [23].

In order to determine the value of series resistance, we analyzed the *I–V* characteristics of the diode using Norde model [24]. According to this model, the series resistance and the barrier height can be determined using the following expressions

$$F(V) = \frac{V}{\gamma} - \left(\frac{kT}{q}\right)\ln\left[\frac{I(V)}{AA^*T^2}\right] \quad (3)$$

where γ is the integer greater than the ideality factor. Here it is taken as 2. The $I(V)$ is the current obtained from the *I–V* characteristic of the diode. Fig. 2 shows the $F(V)$ *vs.* V plot of the fabricated diode. The barrier height was calculated using the expression

$$\phi_b = F(V_o) + \frac{V_o}{\gamma} - \frac{kT}{q} \quad (4)$$

where $F(V_o)$ is the minimum point of $F(V)$ and V_o is the corresponding voltage. The value of barrier height was calculated after getting

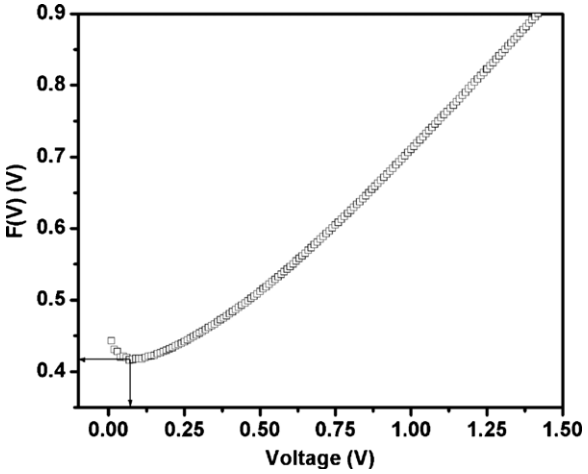

Fig. 2. Norde plot for the Au/3C-SiC/*p*-Si/Al Schottky diode.

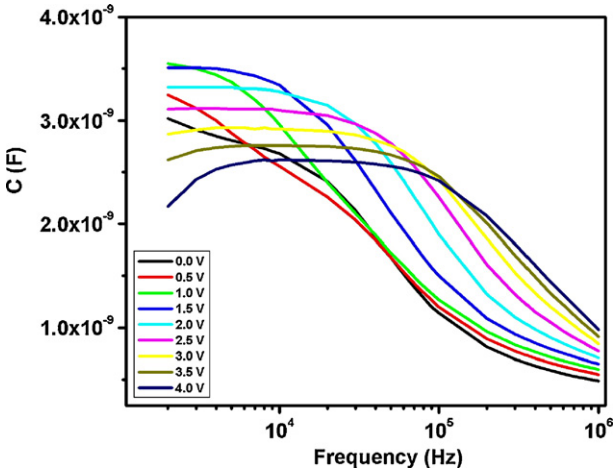

Fig. 4. *C–f* characteristics of the Au/3C-SiC/*p*-Si/Al Schottky diode at various voltages.

minimum of the *F vs. V* plot. The value of series resistance was calculated using the formula

$$R_S = \frac{kT(\gamma - n)}{qI} \tag{5}$$

The values of barrier height and series resistance were obtained to be 0.43 eV and $1.0 \times 10^4\ \Omega$, respectively. The barrier height deduced from the reverse saturation current (0.44 eV) and that deduced by Norde are in agreement with each other. Chung et al. [11] have calculated the barrier height and series resistance of Au/3C-SiC/*n*-Si/Al diode as 0.79 eV and $1.7 \times 10^4\ \Omega$, respectively. The obtained R_S value is quite higher. This can be attributed to the existence of an interfacial insulator layer (SiO_2) at interface of the diode.

3.2. AC impedance study of the Au/3C-SiC/p-Si/Al diode

In Fig. 3, we show the variation of capacitance with applied voltage at different frequencies. As seen in Fig. 3, the capacitance decreases with increase in frequency. Fig. 4 shows the variation of capacitance with frequency at different bias voltages. The decrease in the capacitance at high frequencies depends on the ability of the charge carriers to follow the applied alternating current (*AC*) signal. If the *C–V* measurements were performed at sufficiently higher frequencies, the charge at the interface could not follow the *AC* signal [25]. It is seen in the *C–V* plots that these curves have a peak in low frequency measurements. This peak could be due to the series resistance and change in interface states which are high at low frequency. The observed shift in the peak position at different frequency is due to the fact that the interface states follows the applied *AC* signal, whereas the change in the peak width is related to the number of trapped carriers at interface.

The effect of voltage and frequency on the conductance of the diode was also studied. Fig. 5 shows the conductance–voltage (*G–V*) measurements at different frequencies. As seen in Fig. 5, the conductance of the Au/3C-SiC/*p*-Si/Al diode depends on voltage as well as on frequency. It is observed that the conductance of the diode increases with increase in the frequency. From Fig. 3, it is evident the *C–V* characteristics of the diode shows a non-ideal behavior which may be due to the series resistance, density of the interface states and the formation of insulator layer between the metal and semiconductor. In order to investigate the effect of series resistance on the capacitance and conductance, the corrected capacitance (C_{ADJ}) and corrected conductance (G_{ADJ}) were calculated using the following expressions [26,27]

$$C_{ADJ} = \frac{[G_m^2 + (\omega C_m)^2]C_m}{a^2 + (\omega C_m)^2} \tag{6}$$

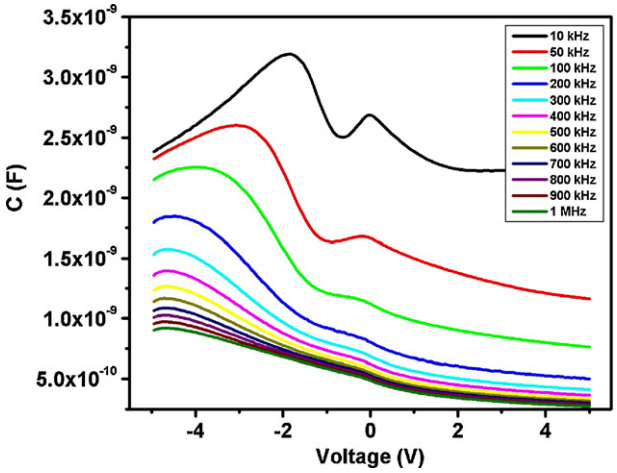

Fig. 3. *C–V* characteristics of the Au/3C-SiC/*p*-Si/Al Schottky diode at various frequencies.

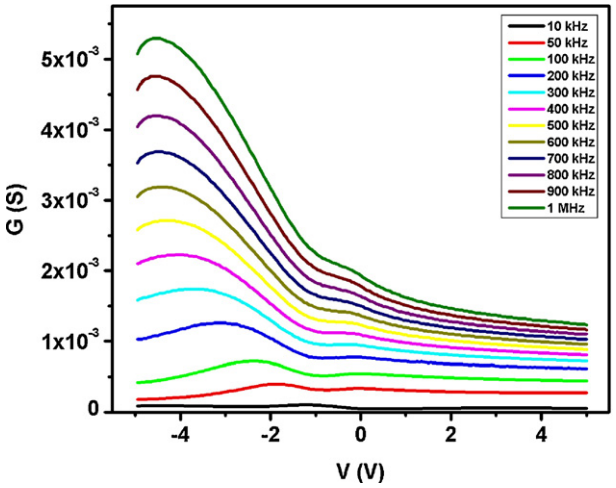

Fig. 5. *G–V* characteristics of the Au/3C-SiC/*p*-Si/Al Schottky diode at various frequencies.

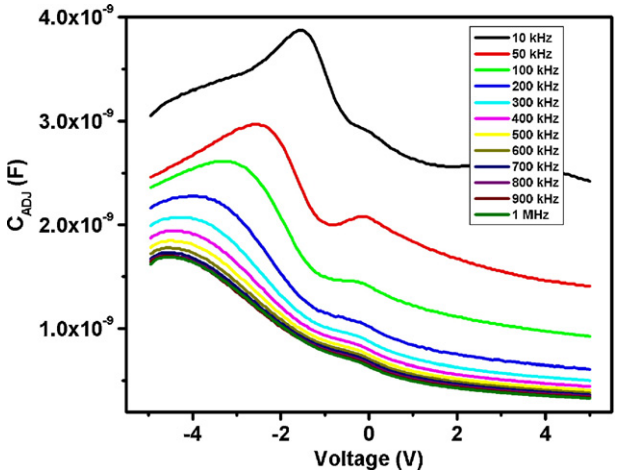

Fig. 6. C_{ADJ}–V characteristics of the Au/3C-SiC/p-Si/Al Schottky diode at various frequencies.

$$G_{ADJ} = \frac{[G_m^2 + (\omega C_m)^2]a}{a^2 + (\omega C_m)^2} \tag{7}$$

where

$$a = G_m - [G_m^2 + (\omega C_m)^2]R_S \tag{8}$$

where C_{ADJ} and G_{ADJ} are series resistance compensated capacitance and conductance, respectively. Figs. 6 and 7 show the C_{ADJ}–V and G_{ADJ}–V plots as a function of frequencies, respectively. It is observed that the C_{ADJ} decreases with increase in frequency, whereas G_{ADJ} increases with increase in frequency. This behavior shows the presence of interface states. At lower frequencies, the higher value of the C_{ADJ} results from the interface states, on the other hand at higher frequencies, the capacitance is not dispersive, as the charge at the interface cannot follow the fast AC signal and they do not contribute to the diode capacitance [28]. In the C_{ADJ}–V and G_{ADJ}–V plots, we observe a peak in the negative bias voltage. And the peaks shift toward the lower negative voltage with decrease in the frequency. These peaks may be due to the presence of interface states and series resistance. The series resistance of the diode was calculated using the following equation

$$R_S = \frac{G_m}{G_m^2 + (\omega C_m)^2} \tag{9}$$

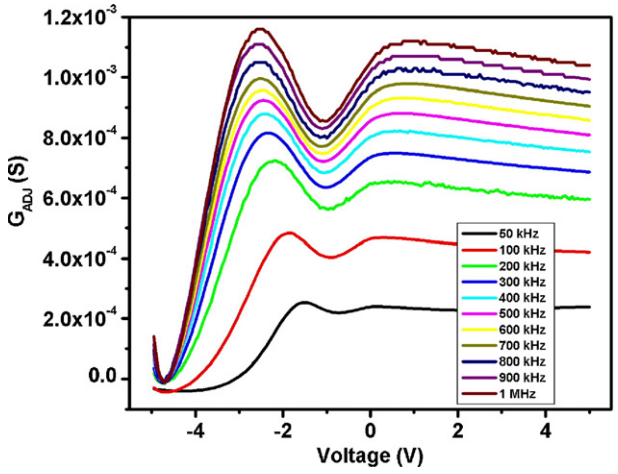

Fig. 7. G_{ADJ}–V characteristics of the Au/3C-SiC/p-Si/Al Schottky diode at various frequencies.

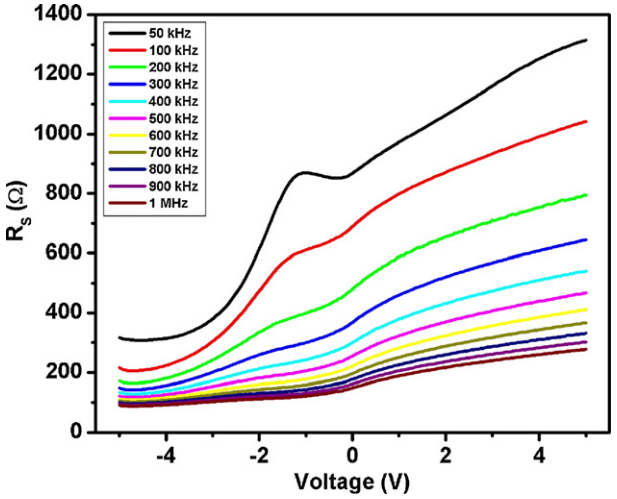

Fig. 8. R_S–V characteristics of the Au/3C-SiC/p-Si/Al Schottky diode at various frequencies.

Fig. 8 shows the R_S–V–f plot of the diode. The R_S–V plots indicate a peak at the lower frequency measurements. It was observed that the peak position shifts with the change in the frequency and the peaks intensity decreases with increasing frequency. The shifting in peak position is due to interface charges following the frequency of applied voltage. The high value of series resistance at low frequencies is because the interface states can follow the AC signal and yield an excess capacitance at low frequency [29]. Bengi et al. [30] have reported that the series resistance of GaAs/AlGaAs single-quantum-well laser diodes decreases and capacitance increases with the increasing temperature which can be attributed to the particular density distribution of interface states and restructuring and reordering of interface charge at metal–semiconductor interface with the increasing temperature.

3.3. Photo-impedance study of the Au/3C-SiC/p-Si/Al diode

The photoresponse of the diode on capacitance, conductance, and series resistance were studied in detail. The transient photocapacitance measurements were investigated at different frequencies under 100 mW/cm^2 illumination intensity (Fig. 9). As evident from Fig. 9, the photocapacitance of the diode increases sharply when the diode is illuminated. The photocapacitance remains almost constant under the illumination. After turning off the illumination, the photocapacitance decreases to almost its initial value. The initial

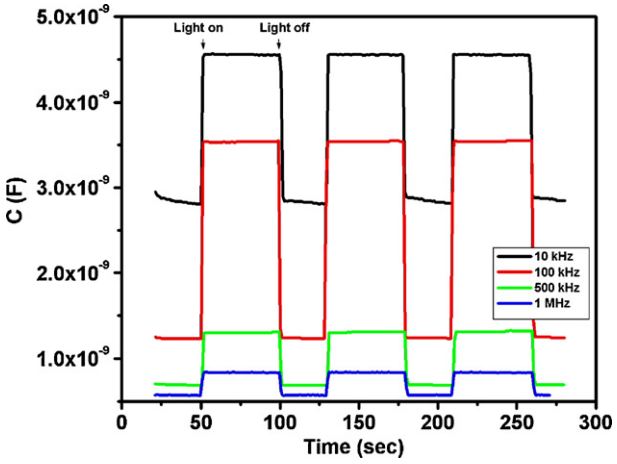

Fig. 9. The transient photocapacitance of the Au/3C-SiC/p-Si/Al Schottky diode.

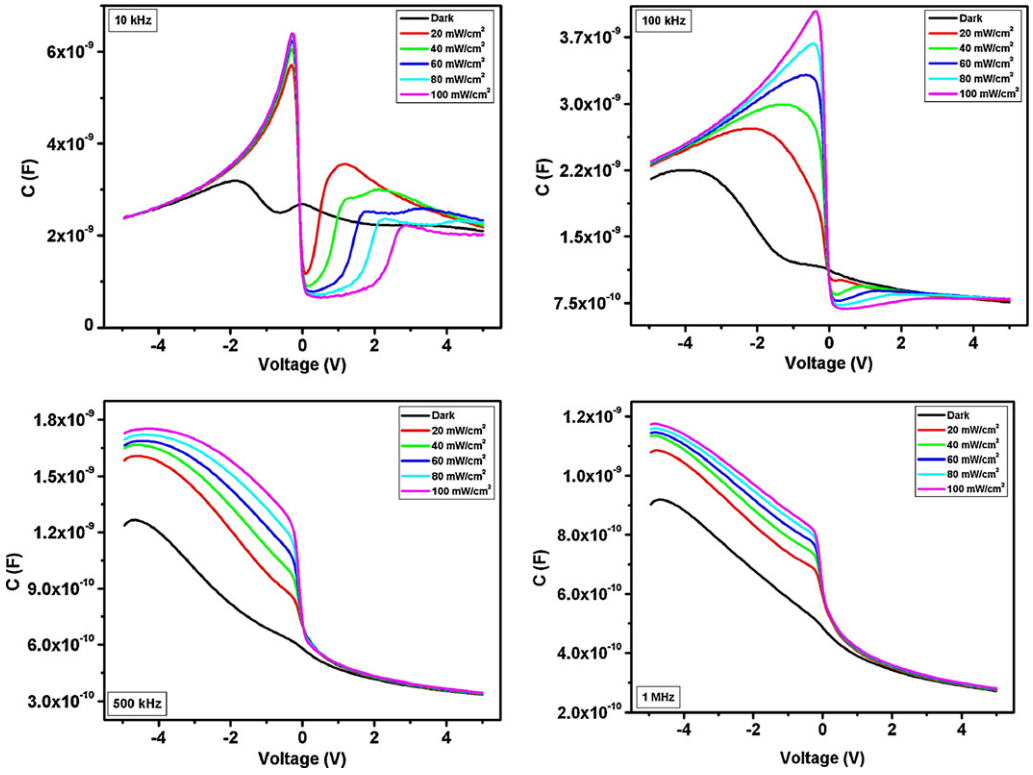

Fig. 10. *C–V* characteristics of the Au/3C-SiC/*p*-Si/Al Schottky diode at various frequencies under dark and illuminations.

rise in the capacitance suggests generation of more free charge carriers at junction on illuminating the diode. The decay of the photocapacitance after switching off the illumination is due to trapping of the charge carriers in the deep levels. This behavior indicates that the fabricated diode exhibits a photocapacitive response. The photocapacitance of the diode depends on the frequency of applied voltage under illumination. As seen in Fig. 9, the change in capacitance with illumination is the highest under 100 kHz due the number of interface charges following the low frequency. Whereas, under 1 MHz, the change in the capacitance with illumination is the lowest due the number of interface charges non-following the high frequency. At the lower frequencies, the interface charges can be rapidly redistributed due to the frequency of applied electric field and in that case, a screening of the field is formed and an overall reduction in the electrical field and this leads to the increase of the capacitance. At the higher frequencies, the interface charges no longer have enough time to rearrange inversions to the applied voltage and so, the capacitance is reached to the minimum value and in that case, the diode does not exhibits a high photocapacitance.

Fig. 10 shows the effect of light illuminations on the *C–V* measurements at different frequencies. As can be seen in Fig. 10, the *C–V* plots show an intersection point at about zero bias voltage. This behavior may be attributed to the lack of free charge charges under illumination. The capacitance of the diode increases with illuminations. The capacitance is almost independent of the light intensity in the reverse bias voltage at low frequency, whereas it became independent of the light intensity in forward bias voltage at higher frequencies. This is due to the presence of interface states. It is also observed that the capacitance increases with increase in the light intensity at higher frequencies. As seen in Fig. 11, the photocapacitance increases linearly with the light intensity at higher frequencies. This suggests that the photocapacitance mechanism of the diode is controlled by shallow traps levels, i.e., the shallow trap levels contribute to the capacitance [31].

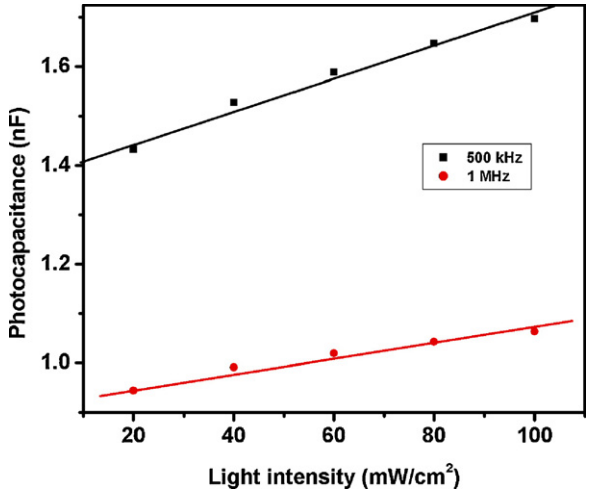

Fig. 11. Variation of photocapacitance with various light intensities at different frequencies.

The effects of light intensity on the properties of conductance at different frequencies are shown in Fig. 12. It was observed that the conductance increases with increase in light intensity in the forward bias voltage at low frequencies, where as it increases with increase in light intensities in the reverse bias voltage at higher frequencies. This is due to the behavior of interface charges, which follow the alternating current signal at lower frequencies and do not follow alternating current signal at higher frequencies. Uslu et al. [32] have studied the effect of illumination on electrical properties of Au/polyvinyl alcohol (Co, Zn doped)/*n*-Si Schottky barrier diode. They observed that the capacitance of the device increases with increase in illumination intensity.

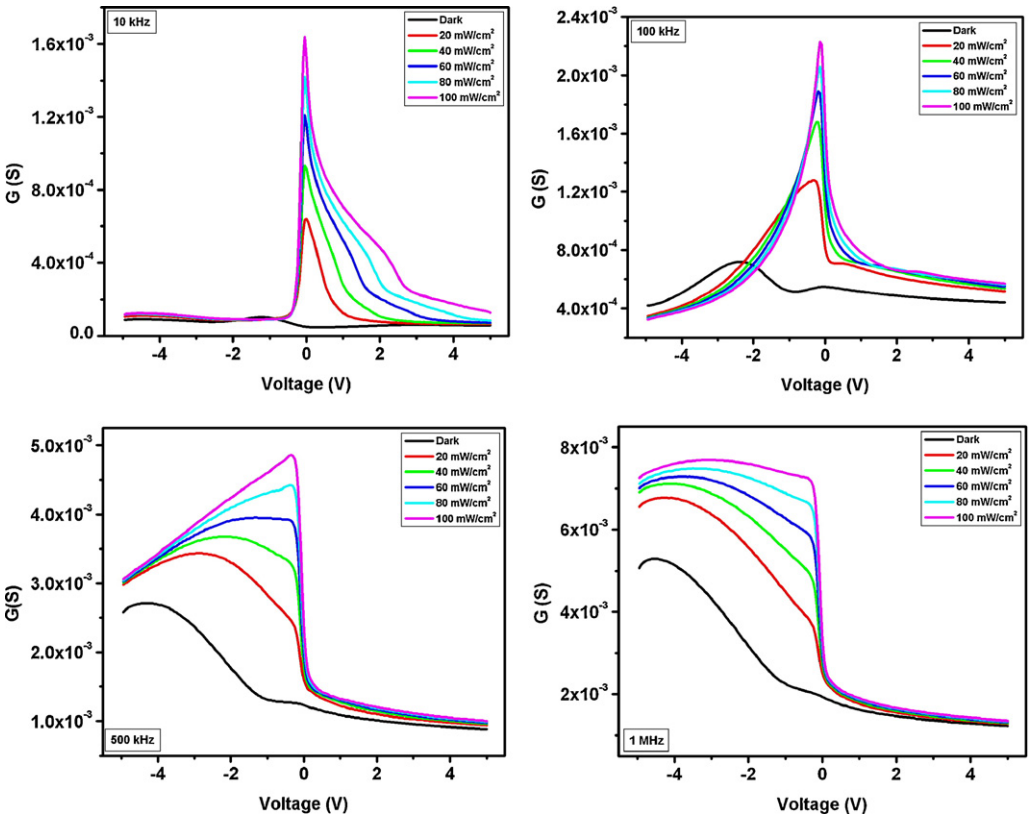

Fig. 12. *G–V* characteristics of the Au/3C-SiC/*p*-Si/Al Schottky diode at various frequencies under dark and illuminations.

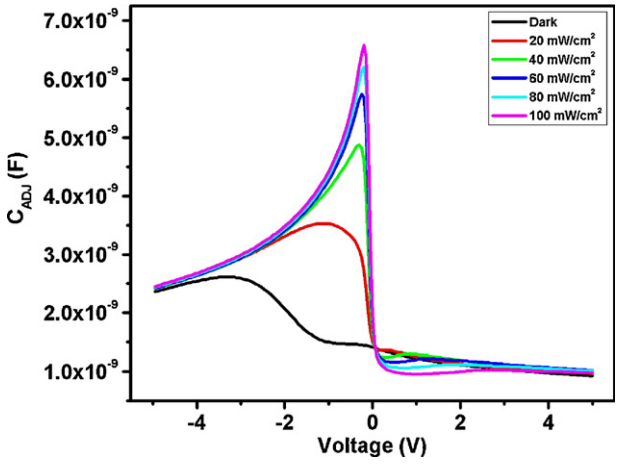

Fig. 13. C_{ADJ}–*V* characteristics of the Au/3C-SiC/*p*-Si/Al Schottky diode at 100 kHz under dark and illuminations.

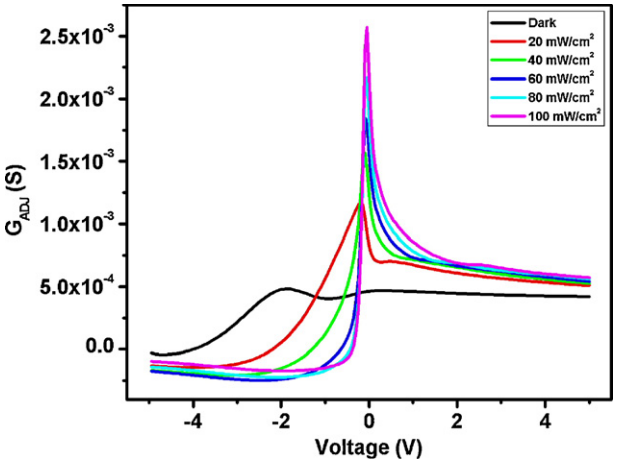

Fig. 14. G_{ADJ}–*V* characteristics of the Au/3C-SiC/*p*-Si/Al Schottky diode at 100 kHz under dark and illuminations.

The effect of series resistance on the photocapacitance and photoconductance has been corrected and the corrected photocapacitance and photoconductance measured at 100 kHz are shown in Figs. 13 and 14, respectively. Fig. 15 shows the effect of light intensity on the series resistance of the diode at different frequencies. As seen in Fig. 15, the series resistance of the diode decreases with increase in frequency and light intensity and R_S–*V* plots exhibit an intersection behavior at point at about zero bias voltage. This behavior may be attributed to the lack of free charges under illumination.

The low series resistance at higher frequencies is explained as the interface states cannot follow the *AC* signal and do not make a contribution to interface states. The low value of series resistance at high light intensity is due to generation of more charge carrier. Illumination intensity effects on the electrical characteristics of Al-TiW-Pd_2Si/*n*-Si Schottky structures have been reported recently [33]. The high values of series resistance at low intensity is explained on the basis of the particular distribution of interface states, surface preparation, inhomogeneity of interfacial layer and barrier height at metal/semiconductor interface.

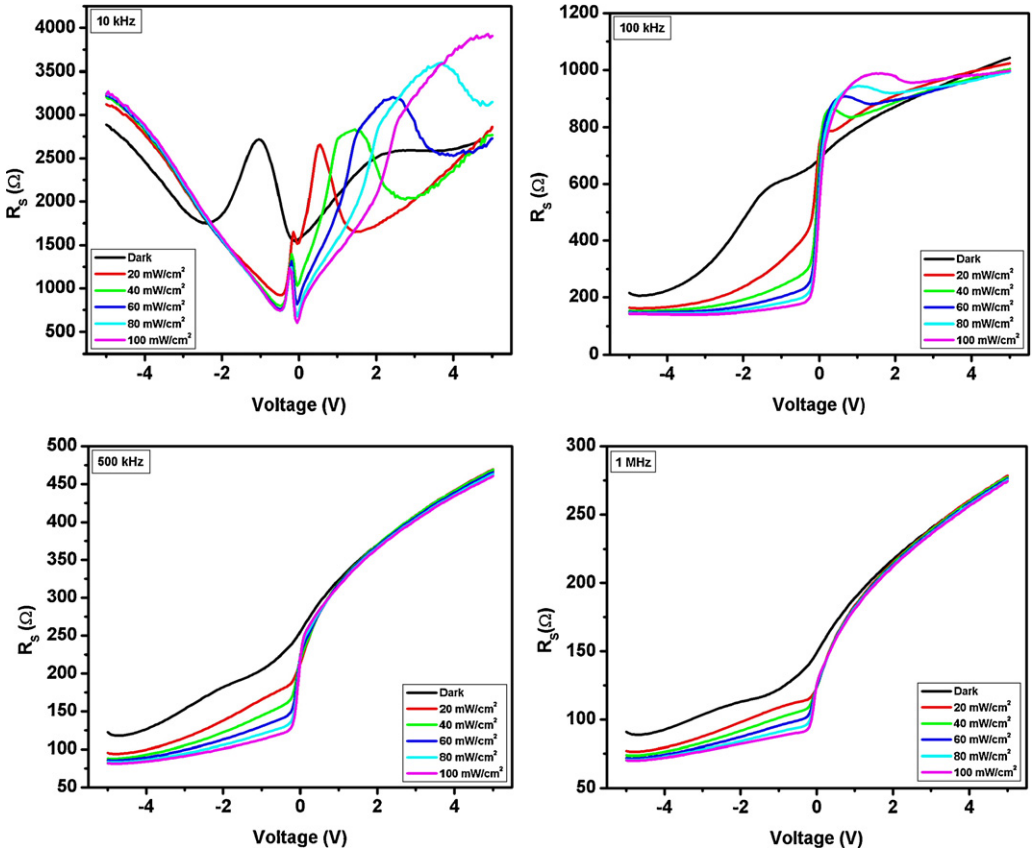

Fig. 15. R_S–V characteristics of the Au/3C-SiC/*p*-Si/Al Schottky diode at various frequencies under dark and illuminations.

4. Conclusions

The device parameters of the Au/3C-SiC/*p*-Si/Al Schottky diode were determined using direct current and impedance measurements. The ideality factor and barrier height of the diode were found to be 1.55 and 0.44 eV, respectively. The transient photocapacitance measurements indicate that the fabricated diode is sensitive to light intensity. The *C*–*V* measurements under different light intensity confirm the photocapacitive properties of the Au/3C-SiC/*p*-Si/Al diode. The low value of series resistance at higher frequencies and light intensities is explained on the basis of interface states and photo generation of charge carriers, respectively.

Acknowledgements

The Global Research Network for Electronic Device and Biosensors (GRNEDB) would like to thank King Saud University for supporting of this project.

References

[1] S.N. Gorin, L.M. Ivanova, Phys. Stat. Sol. (b) 202 (1997) 221.
[2] L. Cao, H. Jiang, H. Song, Z. Li, G. Miao, J. Alloys Compd. 489 (2010) 562.
[3] J. Yi, X.D. He, Y. Sun, J. Alloys Compd. 491 (2010) 436.
[4] K.S. Kim, K.B. Han, G.S. Chung, Physica B 405 (2010) 513.
[5] G.S. Chung, J.H. Ahn, Microelectron. Eng. 85 (2008) 1772.
[6] J. Zhang, C. Carraro, R.T. Howe, R. Maboudian, Surf. Coat. Technol. 201 (2007) 8893.
[7] Y. Ikoma, R. Okuyama, M. Arita, T. Motooka, Thin Solid Films 518 (2010) 3759.
[8] S. Roy, C. Jacob, S. Basu, Solid State Sci. 6 (2004) 377.
[9] T. Mizunami, N. Toyama, Opt. Laser Technol. 35 (2003) 451.
[10] H. Nagasawa, K. Yagi, T. Kawahara, N. Hatta, M. Abe, Microelectron. Eng. 83 (2006) 185.
[11] G.S. Chung, K.S. Kim, F. Yakuphanoglu, J. Alloys Compd. 507 (2010) 508.
[12] Y. Dou, H. Jin, M. Cao, X. Fang, Z. Hou, D. Li, S. Agathopoulos, J. Alloys Compd. 509 (2011) 6117.
[13] K.H. Wu, Y.K. Fang, J.H. Zhou, J.J. Ho, Jpn. J. Appl. Phys. 36 (1997) 5151.
[14] S. Sheng, M.G. Spencer, X. Tang, P. Zhou, K. Wongchotigul, C. Taylor, G.L. Harris, Mater. Sci. Eng. B 46 (1997) 14.
[15] S.M. Sze, Physics of Semiconductor Devices, Wiley, New York, 1979.
[16] R.K. Gupta, R.A. Singh, Mater. Chem. Phys. 86 (2004) 279.
[17] S. Karatas, A. Turut, Nucl. Instrum. Meth. A 566 (2006) 584.
[18] M. Çakar, C. Temirci, A. Türüt, Synth. Met. 142 (2004) 177.
[19] P.L. Hanselaer, W.H. Laflére, R.L. Van Meirhaeghe, F. Cardon, Appl. Phys. A 39 (1986) 129.
[20] F. Yakuphanoglu, Y. Caglar, M. Caglar, S. Ilican, Mater. Sci. Semicond. Proc. 13 (2010) 137.
[21] J. Pezoldt, C. Forster, P. Weih, P. Masri, Appl. Surf. Sci. 184 (2001) 79.
[22] A.A. Lebedev, A.M.S. Chuk, D.V. Davydov, N.S. Savkina, A.S. Tregubova, A.N. Kuznetsov, V.A. Solovev, N.K. Poletaev, Appl. Surf. Sci. 184 (2001) 419.
[23] M.A. Lampert, P. Mark, Current Injection in Solids, Academic Press, New York, 1970.
[24] H. Norde, J. Appl. Phys. 50 (1979) 5052.
[25] F. Yakuphanoglu, S. Okur, Microelectron. Eng. 87 (2010) 30.
[26] E.H. Nicollian, A. Goetzberger, Bell Syst. Technol. J. 46 (1967) 1055.
[27] I. Dokme, S. Altindal, T. Tunc, I. Uslu, Microelectron. Reliab. 50 (2010) 39.
[28] F. Yakuphanoglu, J. Alloys Compd. 494 (2010) 451.
[29] S. Karatas, A. Turut, Vacuum 74 (2004) 45.
[30] A. Bengi, H. Uslu, T. Asar, S. Altındal, S.S. Cetin, T.S. Mammadov, S. Ozcelik, J. Alloys Compd. 509 (2011) 2897.
[31] I.S. Yahia, F. Yakuphanoglu, O.A. Azim, Sol. Energy Mater. Sol. Cells 95 (2011) 2598.
[32] H. Uslu, S. Altındal, I. Dökme, J. Appl. Phys. 108 (2010) 104501.
[33] H. Uslu, S. Altındal, U. Aydemir, I. Dokme, I.M. Afandiyeva, J. Alloys Compd. 503 (2010) 96.